© 2020. Published by The Company of Biologists Ltd | Journal of Cell Science (2020) 133, jcs247379. doi:10.1242/jcs.247379

RESEARCH ARTICLE

Mitochondrial survivin reduces oxidative phosphorylation in cancer cells by inhibiting mitophagy

Amelia R. Townley and Sally P. Wheatley*

ABSTRACT

Survivin (also known as BIRC5) is a cancer-associated protein that is pivotal for cellular life and death – it is an essential mitotic protein and an inhibitor of apoptosis. In cancer cells, a small pool of survivin localises to the mitochondria, the function of which remains to be elucidated. Here, we report that mitochondrial survivin inhibits the selective form of autophagy called 'mitophagy', causing an accumulation of respiratory-defective mitochondria. Mechanistically, the data reveal that survivin prevents recruitment of the E3-ubiquitin ligase Parkin to mitochondria and their subsequent recognition by the autophagosome. The data also demonstrate that cells in which mitophagy has been blocked by survivin expression have an increased dependency on glycolysis. As these effects were found exclusively in cancer cells, they suggest that the primary act of mitochondrial survivin is to steer cells towards the implementation of the Warburg transition by inhibiting mitochondrial turnover, which enables them to adapt and survive.

This article has an associated First Person interview with the first author of the paper.

KEY WORDS: Cancer, Mitochondria, Mitophagy, Respiration, Survivin

INTRODUCTION

Survivin (also known as BIRC5) is a protein at the interface of cellular life and death, as it guides mitosis and inhibits apoptosis (Wheatley and Altieri, 2019). It is overexpressed in cancer cells and is associated with poor patient prognosis (Escuín and Rosell, 1999; reviewed in Jaiswal et al., 2015). Its abundance correlates directly to chemotherapy resistance, highlighting it as a potential anti-cancer target (Morrison et al., 2012). Survivin localises in several distinct pools (Fortugno et al., 2002). During mitosis and as part of the chromosomal passenger complex, it directs chromosome congression and segregation, as well as cytokinesis (Carvalho et al., 2003). When present in interphase, its predominantly cytosolic localisation is key to its anti-apoptotic function (reviewed in Wheatley and Altieri, 2019). The focus of this paper is the mitochondrial pool of survivin, which is found only in cancer cells (Dohi et al., 2004). What survivin does when resident in the mitochondria is a matter of ongoing debate (Hagenbuchner et al., 2013; Rivadeneira et al., 2015), although early evidence suggested that it might be a store of survivin with greater anti-apoptotic potential than the cytosolic pool 'primed' in readiness to respond to pro-apoptotic signals (Dohi et al., 2007).

Malignant transformation requires cellular changes that enable unrestricted proliferation and circumvention of programmes of cell death, such as apoptosis and autophagy. For decades the mitochondrion has been seen as a by-stander of malignant transformation, gaining inactivating mutations from various sources that switch cellular metabolism from oxidative phosphorylation (OxPhos) to glycolysis (Warburg, 1956). More recently it has begun to be appreciated that mitochondria actively participate in driving tumour progression and malignant transformation (Chatterjee et al., 2011; Yadav and Chandra, 2013; van Gisbergen et al., 2015).

Mitochondrial homeostasis, including their quality and length is maintained by the dynamic processes of fusion and fission, which are controlled by factors within the mitochondria and in the cytosol (Westermann, 2010; East and Campanella, 2016). In healthy cells, the balance between fusion and fission is tightly controlled to allow for the timely removal of non-functional mitochondria without affecting respiration (Nunnari et al., 1997). In cancerous cells, this process is commonly deregulated resulting in the gradual accumulation of mitochondrial DNA (mtDNA) mutations that eventually trigger the loss of the respiratory apparatus (Balaban et al., 2005; Porporato et al., 2017), causing a reduction in OxPhos, and greater dependency on glycolysis, hence evoking the 'Warburg effect' (Merz and Westermann, 2009). In normal proliferating cells, fusion is important for the maintenance of healthy mitochondria, as it can rescue damaged mitochondria by mixing their contents with healthy mitochondria (Westermann, 2010). Opposing fusion is fission, a process that generates mitochondrial fragments. In mitosis, fission occurs to ensure that the organelle is correctly inherited (Twig et al., 2008b), but it is also necessary to maintain mitochondrial homeostasis as it precedes the removal of defective mitochondria by the selective form of autophagy, called 'mitophagy' (Twig and Shirihai, 2011; Redmann et al., 2014). Together, with mitochondrial biogenesis, mitophagy is a quality control mechanism that determines mitochondrial mass (Jornayvaz and Shulman, 2010).

Autophagy delivers defective organelles to autophagosomes, which fuse with lysosomes to degrade and recycle their constituents (Youle and Narendra, 2011). Organelles destined for recycling can be delivered to the autophagosome by two distinct pathways, either a ubiquitin-dependent or a ubiquitin-independent pathway (Zaffagnini and Martens, 2016). The ubiquitin-dependent pathway requires ubiquitylation of defunct organelles by E3-ubiquitin ligases and their subsequent recognition by ubiquitin-binding proteins, which enables extension of the pre-autophagosomal (phagophore) membrane and their complete engulfment into the autophagosome (Shaid et al., 2013). Mitochondrial recycling relies upon the action of PTEN-induced kinase 1 (PINK1) and the E3-ubiquitin ligase Parkin (East and Campanella, 2016). Alterations to either of these processes result in the accumulation of defunct,

School of Life Sciences, University of Nottingham, Nottingham NG7 2UH, UK.

*Author for correspondence (sally.wheatley@nottingham.ac.uk)

S.P.W., 0000-0002-9550-8979

Handling Editor: Daniel Billadeau
Received 21 April 2020; Accepted 29 September 2020

Journal of Cell Science (2020) 133, jcs247379. doi:10.1242/jcs.247379

metabolically inactive mitochondria. Reactive oxygen species (ROS), which are a principal cause of mitochondrial DNA (mtDNA) damage, are a by-product of OxPhos. If mitochondria harbouring mtDNA lesions are not removed in a timely manner they can promote tumorigenesis (Ott et al., 2007). Cancer cells typically circumvent the damage by using glycolysis to generate ATP. Even though it is a less efficient means of ATP production, one of its major advantages is that it does not produce ROS, and thus does not cause mtDNA mutations (Vander Heiden et al., 2009). Mitochondrial quality control is a relatively unexplored aspect of cancer, but given the accumulating evidence that alterations in mitophagy can bestow chemotherapy resistance (van Gisbergen et al., 2015), understanding its contribution to the diseased state may reveal an Achilles' heel of cancer (Hagenbuchner et al., 2013; Chourasia et al., 2015; Vara-Perez et al., 2019).

Here, we test the hypothesis that survivin regulates mitochondrial homeostasis and respiratory dependence in cancer cells. We report that, in cancer cells, survivin increases mitochondrial mass and reduces mtDNA quality by inhibiting mitophagy. We propose that, as a consequence of accumulating a high load of respiratory inactive mitochondria, cancer cells with high expression of survivin have a reduced respiratory dependence on OxPhos, forcing them to become more reliant on glycolysis for survival.

RESULTS

Survivin is found in the mitochondria of transformed cells

It has previously been reported that a subpopulation of survivin localises to the mitochondria in cancer cells. To verify that this was the case in the cells being examined here, we carried out subcellular fractionation to enrich for mitochondria in two cancerous lines, HeLa (cervical cancer) and U2OS (osteosarcoma), and in normal fibroblasts (MRC5) (Fig. 1A). All lines were engineered to ectopically express survivin, C-terminally tagged with GFP (survivin–GFP; SVN–GFP) or GFP alone (control). As indicated by enrichment of the voltage-dependent anion channel (VDAC; herein referring to VDAC1), and minimal contamination of tubulin (cytosolic marker) and histone H3 (nuclear marker), survivin–GFP was present in the mitochondria of HeLa and U2OS, but not MRC5 cells. These data corroborate previous work (Dohi et al., 2004), and further demonstrate that survivin is also localised to mitochondria when present at high levels through ectopic expression.

Manipulating survivin expression alters mitochondrial mass

To determine whether mitochondrial survivin can influence mitochondrial mass, we analysed whole-cell extracts (WCEs) of HeLa cells expressing GFP or survivin–GFP by immunoblotting (Fig. 1B) and probed for anti-VDAC as a marker of mitochondrial mass. Semi-quantitative analysis of these blots (Fig. 1C) was carried out by normalising the band intensity of the protein of interest against the anti-tubulin loading control, and is presented as fold change of survivin–GFP compared with GFP. This analysis showed that VDAC levels increased significantly when survivin was expressed. In contrast to the results in HeLa cells, none of these alterations were observed in normal MRC5 fibroblasts expressing survivin–GFP (Fig. 1D,E). To determine whether changes in expression of these proteins could be attributed to changes at the transcriptional level, quantitative PCR (qPCR) was performed on extracts from HeLa cells, and the fold change in expression between survivin–GFP and GFP controls plotted (Fig. 1F). No change in *VDAC* mRNA was observed suggesting that the alterations occurred post-translation.

To further confirm that survivin expression increases mitochondrial mass, we quantified mitochondrial DNA (mtDNA) copy number. Genomic DNA was extracted from HeLa or MRC5 cells expressing either GFP or survivin–GFP, or after siRNA depletion. qPCR was used to determine the abundance of the mtDNA-encoded tRNA(LEU) gene, which was then compared to the stably expressed nuclear reference genes *ACTB* (actin) and *TUBB* (tubulin). The fold change of RNA between cells expressing survivin–GFP and GFP was then calculated and presented on a $\log_2$ scale. Survivin overexpression increased mtDNA tRNA(LEU) gene expression in HeLa cells (Fig. 1G), and decreased it in MRC5 cells (Fig. 1H). Thus, by an independent method, these data concur that mitomass is elevated by survivin expression in HeLa, but not MRC5 cells.

Having established that survivin overexpression increases mitomass, we next asked whether depleting it would have the opposite effect. To investigate this survivin-specific siRNA was transfected (48 h) in HeLa and MRC5 cells (Fig. S1). WCEs were separated by SDS-PAGE, transferred to nitrocellulose and probed for VDAC as a mitochondrial marker. Semi-quantitative analysis of blots was used to determine the fold change in siRNA-treated versus untreated cells, normalised to tubulin. Survivin depletion caused a significant reduction in VDAC (Fig. S1A,B). By contrast none of these effects were observed in MRC5 cells (Fig. S1C,D). These data complement the overexpression data, and collectively prove that changes in survivin expression alter mitochondrial mass in some cancerous cells, but not in normal fibroblasts.

To determine whether the increase in mitomass was caused by elevated mitochondrial biogenesis, HeLa and MRC5 WCEs expressing GFP or survivin–GFP were run on an SDS-PAGE gel, and immunoblotted for the biogenesis marker PGC1α (also known as PPARGC1A) (Fig. 1I,K). Semi-quantitative analysis showed that protein expression was decreased in HeLa cells (Fig. 1J) and not altered in MRC5 cells (Fig. 1L). Thus, we conclude that the observed increase in mitomass is not due to increased mitochondrial biogenesis.

Finally, to determine whether mitochondrial survivin influences the expression of mitochondrial protein associated with fission or fusion, we analysed WCEs of HeLa cells expressing GFP or survivin–GFP by immunoblotting (Fig. S1E) and probed for fission proteins DRP1 (also known as DNM1L) and FIS1, as well as the fusion proteins OPA1, MFN1 and MFN2, using tubulin as a loading control and VDAC as a marker of mitochondrial mass. Semi-quantitative analysis was calculated as described above and presented as the fold change of survivin–GFP compared with GFP (Fig. S1F). This analysis demonstrated a statistical increase in DRP1, OPA1 and MFN2 expression, which was removed when the data were normalised to VDAC to account for mitochondrial mass alterations (Fig. S1G). A statistical decrease in FIS1 expression was still observed when normalised to VDAC, demonstrating a potential mitomass-independent alteration to FIS1 levels. None of these changes were observed in normal MRC5 fibroblasts expressing survivin–GFP (Fig. S1H,I). Collectively, these data demonstrate that the observed increase in mitomass observed in HeLa cells cannot be attributed to changes in the expression of fission and fusion factors associated with mitochondrial dynamics. Survivin does not alter mitochondrial morphology or polarisation in HeLa cells.

Next, to clarify whether alterations to mitomass are caused by changes to mitochondrial dynamics, we used a combination of fluorescent mitochondrial stains and live imaging to observe the total mitochondrial network in HeLa cells transiently overexpressing GFP or RFP, or survivin–GFP or survivin–RFP (SVN–RFP) and labelled with MitoTracker Red (Fig. 1M; colour in

Journal of Cell Science (2020) 133, jcs247379. doi:10.1242/jcs.247379

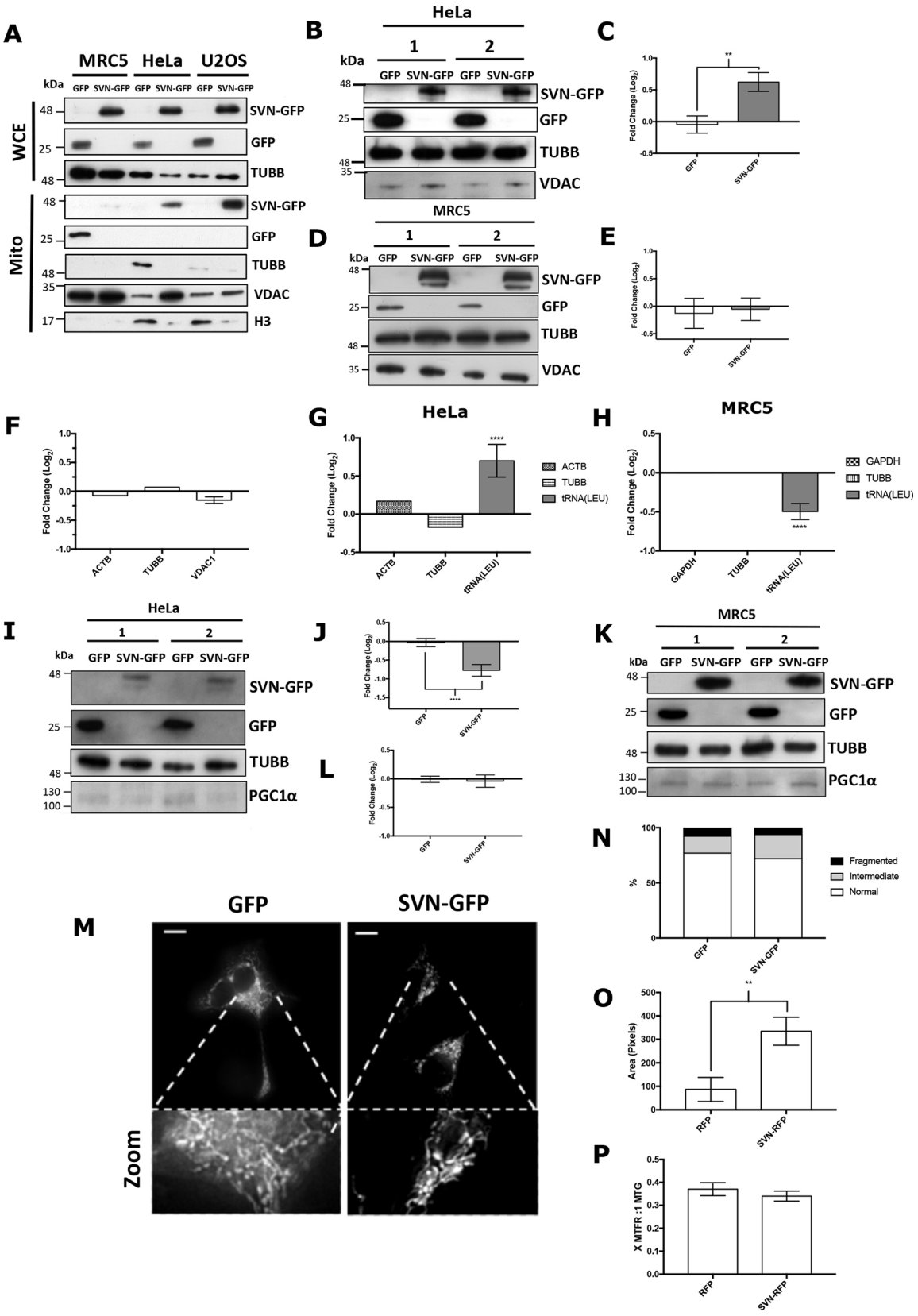

Fig. 1. See next page for legend.

Fig. S2) to visualise the mitochondrial network and found no gross abnormalities in terms of their overall appearance, categorised as normal or fragmented (Fig. 1N). However, consistent with the immunoblotting and qPCR data, when MitoTracker Green was used to measure total pixel area in RFP- and survivin–RFP-expressing cells it was apparent that mitochondrial area was significantly higher in survivin-expressing cells (Fig. 1O). Note that GFP and RFP labels were used interchangeably, and selected due to availability of

Journal of Cell Science (2020) 133, jcs247379. doi:10.1242/jcs.247379

Fig. 1. Survivin up-regulation increases mitochondrial mass independent of altered mitochondrial biogenesis or dynamics. (A) Immunoblot of the mitochondria-enriched fractions (Mito) from GFP and survivin–GFP (SVN–GFP) overexpressing MRC5, HeLa and U2OS cells. WCEs are included in the lower panel to indicate equality in expression of each ectopic protein. VDAC is a mitochondrial (OMM) marker; histone 3 (H3) indicates any nuclear contamination, and tubulin serves both an indicator of cytoplasmic contamination (Mito) and a loading control (WCE). (B–E) Immunoblot analysis of VDAC protein expression in WCEs from HeLa sublines indicated, probed with tubulin as a loading control. Compared to GFP controls SVN–GFP-expressing cells had increased VDAC expression. (C) Semi-quantitative analysis of results in B; n=3. Pixel intensity was normalised to tubulin, and presented as fold change ($\log_2$ scale) compared to the GFP control. $^{**}P$<0.01 (two-way ANOVA). (D) Experiment described in B carried out in MRC5 cells. (E) Semi-quantitative analysis of results in D normalised to tubulin as in C; n=3. Two-way ANOVA shows no statistical differences in protein expression caused by SVN–GFP expression. (F) qPCR analysis of VDAC expression in HeLa cells overexpressing GFP or SVN–GFP. *VDAC* mRNA remains constant with SVN–GFP expression. (G,H) mtDNA copy number was determined by qPCR analysis on genomic DNA extracted from (G) HeLa and (H) MRC5 cells expressing GFP or SVN–GFP. The mitochondrial encoded tRNA(LEU) gene was quantified and compared to two stably expressed nuclear reference genes, tubulin (*TUBB*) and actin (*ACTB*) or *GAPDH*. tRNA(LEU) was increased and decreased in SVN-GFP expressing HeLas and MRC5 cells, respectively. $^{****}P$<0.0001 (Statistical analysis performed in REST software using Pfaffl method.). (I) Immunoblotting of WCEs from HeLa or (K) MRC5 cells overexpressing GFP or SVN–GFP. Membranes were probed for PGC1α as a mitochondrial biogenesis marker and tubulin as a loading control, n=3 (with internal triplicates). (J,L) Semi-quantification of immunoblots in I and K, respectively, presented as fold change ($\log_2$ scale) compared to the GFP control. SVN–GFP expression in HeLa cells reduces the expression of PGC1α but causes no alterations in MRC5 cells. $^{****}P$<0.0001 (two-way ANOVA). (M,N) HeLa cells expressing GFP or SVN–GFP were stained with 250 nM MitoTracker Red FM and imaged live; three mitochondrial phenotypes were observed: normal, intermediate or fragmented. A Chi-squared test indicated a similar mitochondrial distribution in both lines regardless of survivin status, n=3, d.f.=2. Full galleries are shown in Fig. S2. Scale bars: 15 µm. (O,P) HeLa cells transiently expressing RFP or SVN–RFP were stained with MitoTracker Green (MTG) or MitoTracker Far Red (MTFR) and imaged live. Images were thresholded using Fiji software, mean pixel intensity and area was quantified and MTFR signal normalised to MTG; n=3. Survivin overexpression does not alter mitochondrial membrane potential in HeLa cells but does increase mitochondrial pixel area. $^{**}P$<0.01 (two-way ANOVA). All quantitative results are mean±s.e.m.

relevant MitoTracker dyes. We then monitored alterations to mitochondrial membrane potential using MitoTracker Far Red, a fluorescent stain that highlights polarised mitochondria specifically. The average signal intensity was quantified and normalised to that of MitoTracker Green to account for mitochondrial mass (MTFR: MTG). As shown in Fig. 1P, in HeLa cells, mitochondrial polarisation was not affected by survivin expression. Thus, we conclude that survivin expression causes an increase in mitomass as judged by the area that they cover but that the mitochondria held their membrane potential.

Forced mitochondrial localisation of survivin in normal fibroblasts increases mitomass

To assess whether the effects to mitomass were due specifically to the mitochondrial localisation of survivin, we utilised a survivin–GFP construct tagged with a bona fide mitochondrial-targeting sequence (MTS) from cytochrome *c* oxidase subunit VIIIA, thus, forcing survivin to be localised to mitochondrial in normal fibroblasts (Fig. 2A). Immunoblots of WCEs from MRC5 cells expressing GFP, SVN–GFP or MTS-survivin–GFP (MTS-SVN–GFP) were probed for anti-VDAC to assess mitochondrial mass, and PGC1α to assess alterations to mitochondrial biogenesis (Fig. 2B). Semi-quantitative analysis of protein expression normalised to tubulin showed that forced mitochondrial localisation of survivin in MRC5 cells significantly increased VDAC expression (Fig. 2C), without altering expression of the mitochondrial biogenesis protein PGC1α (Fig. 2D). This suggests that mitochondrial localisation of survivin can account for an increase in mitochondrial mass.

Survivin does not inhibit mitophagic steps preceding mitochondrial translocation of Parkin

As the experiments described thus far suggest that survivin increases mitochondrial mass independently from mitochondrial biogenesis or dynamics, we next asked whether changes to the selective autophagic process of mitophagy could be responsible. Defective regions of the mitochondrial network with depolarised membranes, due to their inactivity, are selected for degradation by the process of mitochondrial fission. Mitophagy is then triggered by the accumulation of full-length PINK1 spanning the outer mitochondrial membrane (OMM), which phosphorylates both OMM protein targets as well as the E3-ubiquitin ligase Parkin, causing its translocation from the cytosol to the OMM (see Introduction).

To discover where survivin operates in the mitophagic pathway, first HeLa cells expressing GFP or survivin–GFP, or RFP or survivin–RFP were treated with FCCP (10 µM) to depolarise the mitochondria and stimulate mitophagy. To ensure that the effects were mitophagy specific and that there was no influence from apoptotic activity, the experiment was carried out over 3 h (see Dispersyn et al., 1999). Cells were then stained with MitoTracker Red to visualise the mitochondrial network, and MitoTracker Green or MitoTracker Far Red to determine membrane polarisation, respectively. As shown in Fig. 3A,B, FCCP induced mitochondrial fission similarly in both cell lines, demonstrating that survivin cannot stop chemically triggered mitochondrial fragmentation. Under these conditions, survivin expression also did not prevent OMM depolarisation (Fig. 3C).

Next, to determine whether survivin alters PINK1 stabilisation, HeLa, U2OS or MRC5 cells were treated with FCCP (10 µM) and chloroquine (CQ; 100 µM) for 6, 12 or 24 h, WCE were prepared and immunoblots probed for PINK1 to determine its stability post mitophagy stimulation (Fig. 3D,F,H). Semi-quantification revealed no alterations to PINK1 stabilisation over the time course in any of the cell lines (Fig. 3E,G,I). Finally, to determine whether survivin alters the interaction of PINK1 and its target E3-ubiquitin ligase Parkin, we performed a pulldown with recombinantly expressed GST–Parkin in the presence of a HeLa WCE expressing GFP or survivin–GFP (Fig. 3J). Immunoblotting of the GST-pulldown assay shows survivin does not alter the interaction of PINK1 and GST–Parkin.

Survivin prevents Parkin recruitment to the mitochondria

We then asked whether survivin alters the recruitment of Parkin to the mitochondria post mitophagy stimulation. To address this, HeLa and MRC5 cells were transiently transfected with the mitophagy-specific E3-ligase Parkin, N-terminally tagged with mCherry, and FCCP treated, then labelled with MitoTracker Far Red and analysed by fluorescence imaging. Here, a marked difference was seen; mCherry–Parkin was recruited to the mitochondria of GFP–HeLa cells after FCCP treatment, but it was retained in the cytoplasm in survivin–GFP cells (Fig. 4A), and this trend was confirmed by phenotype counting and quantification (Fig. 4B). Conversely, the mitochondrial recruitment of mCherry–Parkin was unaffected in MRC5 cells expressing survivin–GFP (Fig. S3, quantification shown in Fig. 4C). From this, we conclude that after mitochondrial

Journal of Cell Science (2020) 133, jcs247379. doi:10.1242/jcs.247379

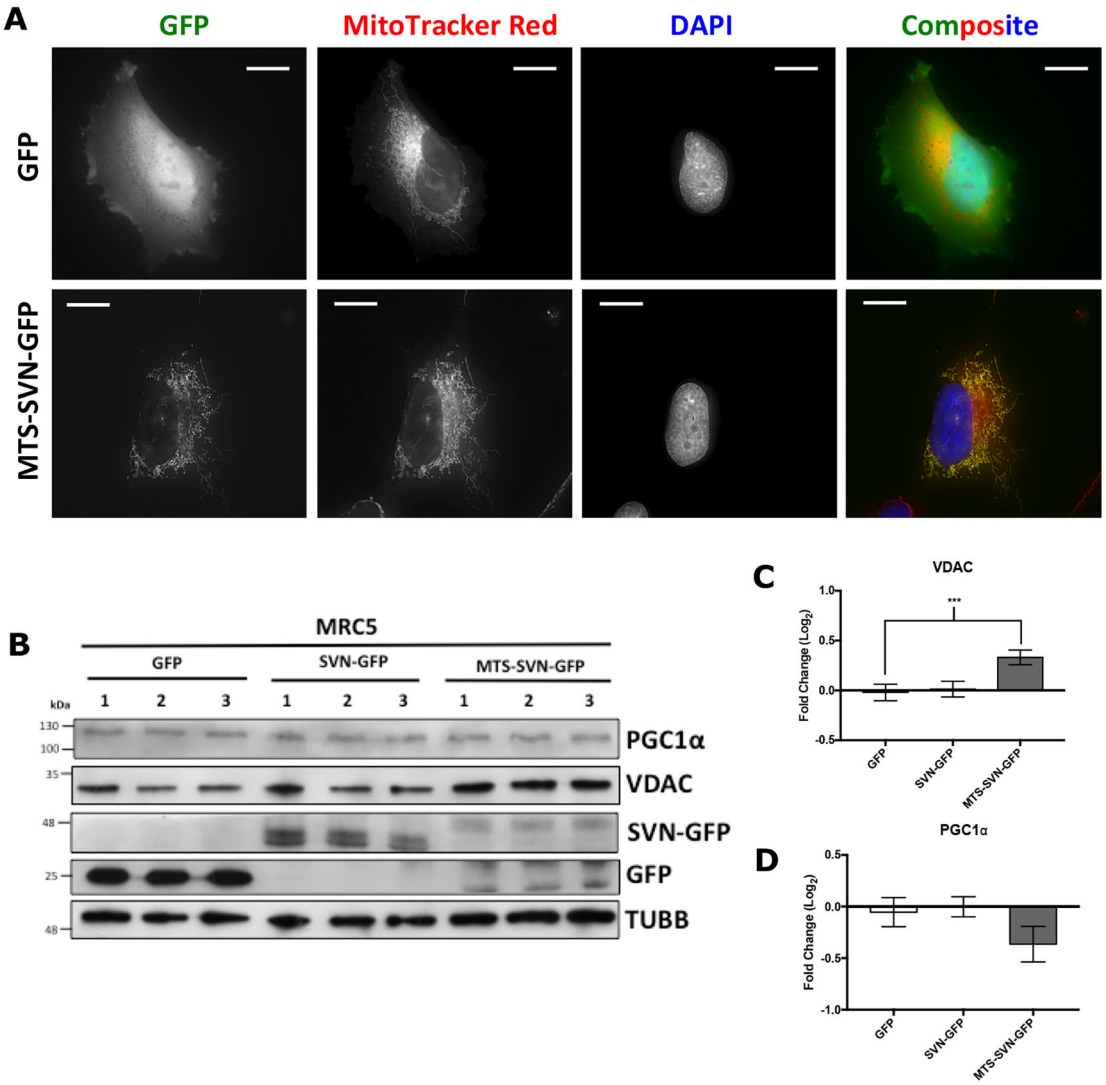

Fig. 2. Mitochondrial localisation of survivin is required for mitochondrial mass alterations. (A) MRC5 cells expressing GFP, survivin–GFP (SVN–GFP) or MTS-survivin–GFP (MTS-SVN–GFP) were stained with 250 nM MitoTracker Red FM and NucBlue, then imaged live to prove MTS-SVN–GFP forces the mitochondrial localisation of survivin in non-cancerous normal fibroblasts. Scale bars: 15 µm. (B) Immunoblot analysis of PGC1α and VDAC protein expression in WCEs from MRC5 sublines indicated, probed with tubulin as a loading control. Compared to GFP controls MTS-SVN–GFP expressing cells had increased VDAC expression, and showed no alterations to PGC1α expression. (C,D) Semi-quantitative analysis of results in B. Pixel intensity of each respective protein was normalised to tubulin, and presented as fold change (log2 scale) compared to the GFP control. Results are mean±s.e.m. (*n*=3). ***P<0.001 (two-way ANOVA).

fragmentation and depolarisation, survivin prevents Parkin recruitment from the cytosol to the mitochondria, which blocks mitophagy in cancer cells.

Survivin decreases mitochondrial colocalisation with lysosomes after mitophagy stimulation

To further confirm how survivin affects mitophagy, HeLa cells expressing RFP or SVN–RFP were treated with FCCP as described above, and stained with LysoTracker Blue to observe autophagosomes, and MitoTracker Green to observe mitochondria (Fig. 5A; see Fig. S4 for full gallery). Colocalisation analysis was then carried out to assess the proportion of the mitochondrial network that colocalised with lysosomes. This demonstrated that post FCCP treatment, significantly more mitochondria and lysosomes colocalised in RFP-expressing cells than in SVN–RFP cells, as shown by pixel intensity line plots (Fig. 5B, arrows, and 5C) and whole pixel colocalisation analysis of images (Fig. 5D).

Survivin mimics the effect of Bcl-2 upon mitophagy

Having established that mitochondrial survivin increases mitomass by inhibiting mitophagy, we next asked whether survivin cooperates with the apoptotic collaborator Bcl-2 in this process. To address this, HeLa cells expressing GFP or survivin–GFP were treated with the Bcl-2 inhibitor Navitoclax (1 µM) and 10 µM FCCP to stimulate mitophagy post transfection with mCherry–Parkin. Here, mCherry–Parkin translocation to the mitochondrion was increased after FCCP treatment with Navitoclax in cells expressing survivin–GFP, but not in GFP-expressing cells (Fig. S5A, quantified in S5B). A UV dose–response curve was simultaneously plotted to prove that Navitoclax (1 µM) was sufficient to inhibit Bcl-2 activity (Fig. S5C). From these data, we conclude that the effect of survivin on mitophagy might be enhanced via collaboration with Bcl-2.

Survivin compromises mtDNA integrity

As the role of mitophagy is to eliminate defective mitochondria, we next examined the quality of accumulated mtDNA using a

Journal of Cell Science (2020) 133, jcs247379. doi:10.1242/jcs.247379

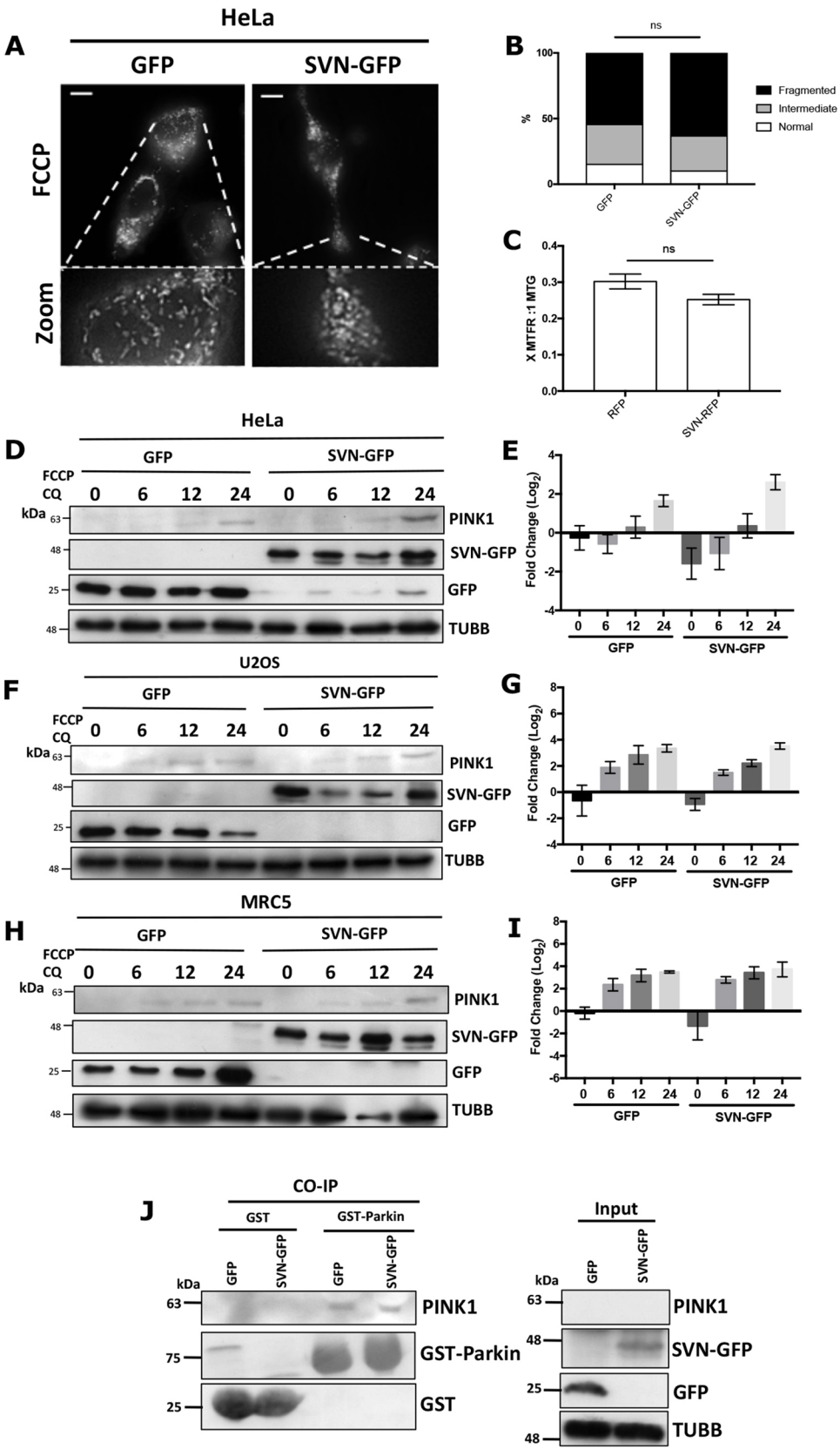

Fig. 3. Survivin does not interfere with mitophagic stages preceding Parkin mitochondrial translocation. (A,B) HeLa cells were treated with 10 µM FCCP for 6 h, stained with 250 nM MitoTracker Red and imaged live. Mitochondrial distribution was scored as normal, fragmented, or intermediate, and no significant (ns) difference between cells expressing GFP or survivin–GFP (SVN–GFP) was seen (Chi-squared test, n=3, d.f.=2). Scale bar: 15 µm. (C) HeLa cells transiently transfected with cDNA for RFP or SVN–RFP were treated as in A, and mitochondrial membrane potential measured using MitoTracker Far Red (MTFR), and expressed as a ratio to MitoTracker Green (MTG). SVN–GFP expression did not alter MTFR signal intensity, indicating no alterations to mitochondrial membrane potential. (D,F,H) HeLa, U2OS and MRC5 cells were treated with 10 µM FCCP and 100 µM CQ for 6, 12 and 24 h, and WCEs prepared and analysed by immunoblotting. Membranes were probed for expression of the kinase PINK1 and GFP to confirm cell line expression, and tubulin was used as a loading control; n=3 (with internal triplicates). SVN–GFP expression does not alter PINK1 stabilisation post mitophagy stimulation. (E,G,I) Semi-quantification of immunoblots in D, F and H, respectively, presented as fold change ($\log_2$ scale) compared to the GFP control time 0; n=3, d.f.=32 (with internal triplicates). No statistical alterations are observed (two-way ANOVA). (J) GST pulldown assay of purified GST–Parkin and GST alone using WCE made from HeLa GFP or SVN–GFP cells. Samples were analysed by immunoblotting, and membranes probed for GST to confirm pulldown, GFP to check expression in WCEs, and PINK1 to assess success of pulldown. Tubulin was used as a loading control. SVN–GFP does not prevent the interaction of GST–Parkin with PINK1; n=3. All quantitative results are mean±s.e.m.

PCR-based lesion frequency assay. Briefly, genomic DNA was prepared from cells as described for Fig. 1G,H, and PCRs were carried out to produce either a ‘long read’ (9 kb) or a ‘short read’ (150 bp) product. In this lesion assay, if mtDNA is intact both products will be generated; however, if the DNA polymerase encounters lesions, it will stall and less 9 kb product will form. The 150 bp product is used as a loading control. As shown in Fig. 6A, less 9 kb product was generated in HeLa cells expressing survivin

Journal of Cell Science

Journal of Cell Science (2020) 133, jcs247379. doi:10.1242/jcs.247379

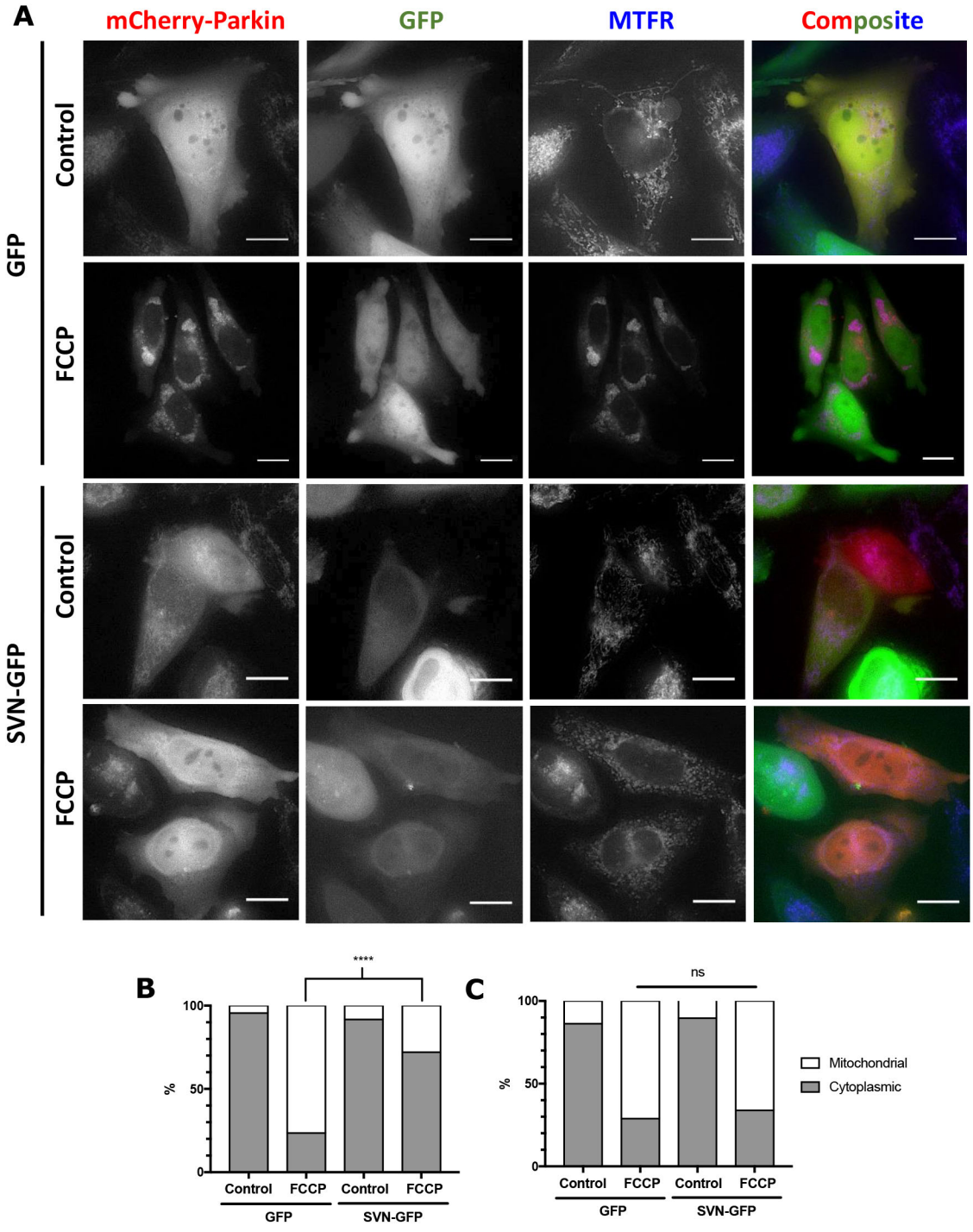

Fig. 4. Survivin prevents mitochondrial recruitment of mCherry-Parkin. (A) HeLa or (C) MRC5 cells were treated with 10 µM FCCP post-transfection with cDNA encoding mCherry–Parkin and stained with NucBlue to visualise nuclei. Representative images, thresholded using Fiji software are shown. Scale bars: 15 µm. A full MRC5 figure shown in Fig. S3. (B,C) Cells were counted for mitochondrial or cytoplasmic localisation of mCherry–Parkin, and a Chi-squared test performed to analyse differences in phenotypes. (B) In HeLa cells, Parkin relocates to the mitochondria in GFP cells treated with FCCP, but remains cytoplasmic in SVN-GFP cells; n=3. (C) No alterations were observed in mCherry–Parkin translocation in MRC5 cells. Results are mean±s.e.m. ****P<0.0001; ns, not significant.

compared to the GFP control, a difference that, when normalised to the 150 bp was highly significant (Fig. 6B). Conversely the 9 kb product was not only retained but actually increased upon survivin depletion from HeLa cells (Fig. 6C,D). In contrast, in MRC5 cells depleting survivin had no effect (Fig. 6E,F). Taken together, these data suggest that survivin reduces the quality of mtDNA specifically in cancer cells.

Survivin expression phenocopies chloroquine treatment and reduces oxidative phosphorylation in cancer cells

Based on the observations presented thus far, we hypothesised that survivin inhibits the removal of defective mitochondria by mitophagy, reducing overall mitochondrial quality. To test this, cells overexpressing GFP or survivin–GFP were exposed to the autophagy inhibitor CQ for 16 h, the mitochondria isolated and a

Journal of Cell Science (2020) 133, jcs247379. doi:10.1242/jcs.247379

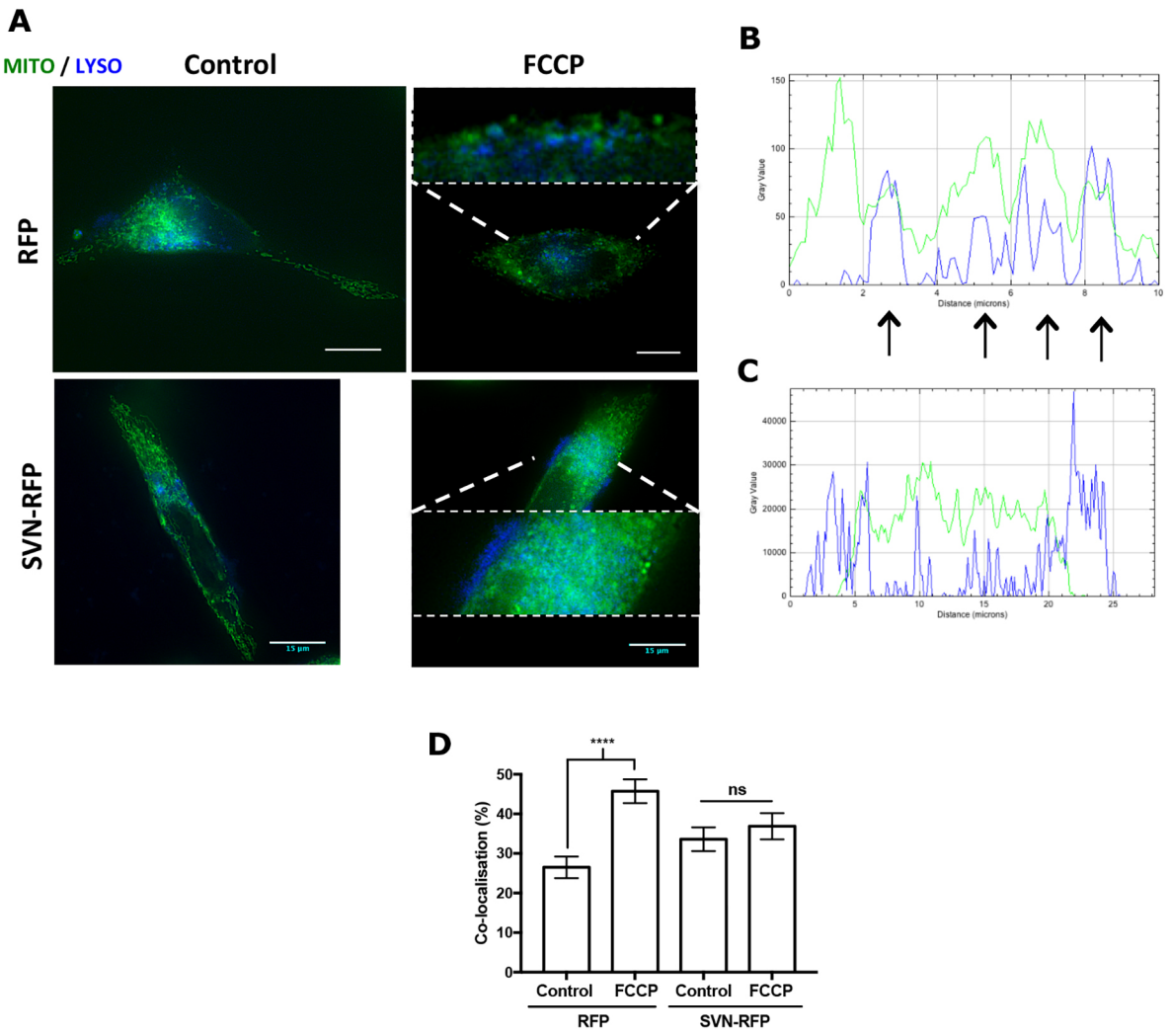

Fig. 5. Mitochondrial colocalisation with lysosomes is reduced in survivin–RFP-expressing HeLa cells. (A) HeLa cells were treated with 10 µM FCCP post-transfection with cDNA encoding RFP or survivin–RFP (SVN–RFP) and stained with 75 nM LysoTracker Blue to visualise lysosomes and 250 nM MitoTracker Green for mitochondria. Representative images, thresholded using Fiji Software, are shown. Magnified sections show colocalisation of mitochondria and lysosomes. Full figure shown in Fig. S4. Scale bars: 15 µm. (B,C) Pixel intensity profile plots over a line draw through a section of RFP (B) and survivin–RFP (C) cells treated with FCCP. RFP cells show a colocalisation of LysoTracker Blue and MitoTracker Green peaks (arrows). (D) Fiji colocalisation analysis of MitoTracker Green and LysoTracker Blue pixels, shown as percentage colocalisation. There is a significant increase in colocalisation after FCCP treatment of RFP cells, but no alteration to survivin–RFP cells. Results are mean±s.e.m.; n=3. ****P<0.0001; ns, not significant (one-way ANOVA).

resazurin assay performed to assess their respiration. As shown in Fig. 7A–D, CQ treatment (50 and 150 µM) reduced metabolism of mitochondria isolated from GFP-expressing HeLa or U2OS cells, which is consistent with a block on the removal of defunct mitochondria. By contrast, mitochondria isolated from survivin–GFP cells, showed reduced respiration in the absence of CQ. After CQ exposure, this survivin-induced suppression of metabolism did not reduce further, but actually showed a slight elevation, for reasons that remain unclear. Consistent with the lack of survivin in the mitochondria of normal cells, there was no significant difference in the respiratory profiles of mitochondria isolated from MRC5 GFP or survivin–GFP cells, which responded similarly to CQ (Fig. 7E,F). Taken together, these data suggest that survivin expression in cancer cells represses mitochondrial metabolism and phenocopies CQ treatment.

Having shown that mitochondrial quality is impaired by survivin upregulation, we next asked directly whether survivin expression affected mitochondrial oxidative phosphorylation. To address this. a resazurin assay was carried out every 30 min over 4 h on mitochondria isolated from HeLa, U2OS or MRC5 cells (Fig. 8). Both HeLa and U2OS cells expressing survivin–GFP showed a significant decrease in resorufin fluorescence compared to GFP-expressing cells (Fig. 8A,C). To ensure the observed alterations were most likely due to changes in OxPhos rather than the mitochondrial TCA cycle, we also determined the response of each line to the complex V inhibitor oligomycin (Fig. 8B,D,F). Mitochondria isolated from both HeLa and U2OS cells expressing GFP were more sensitive to oligomycin than those from survivin–GFP cells (Fig. 8B,D), suggesting that survivin significantly reduced OxPhos in cancer cells. In contrast, no significant difference was seen in the ability of MRC5-derived mitochondria to metabolise resazurin (Fig. 8E; Fig. S6). Furthermore, forced mitochondrial localisation of survivin in MRC5 cells using MTS-SVN–GFP, was able to reduce mitochondrial metabolism in the same manner as in SVN–GFP expressing HeLa and U2OS cells (Fig. 8F). From these data, we conclude that survivin can inhibit reduction reactions when present within mitochondria.

Journal of Cell Science (2020) 133, jcs247379. doi:10.1242/jcs.247379

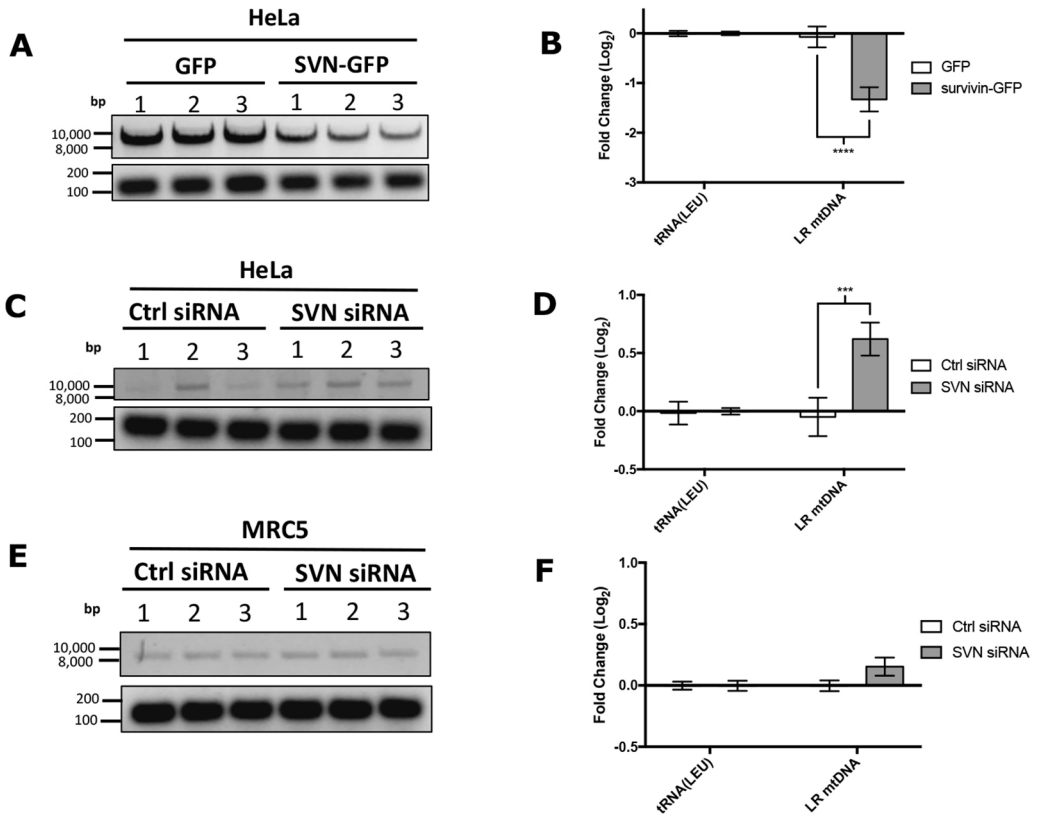

Fig. 6. mtDNA quality decreases in HeLa cells overexpressing survivin. (A,C,E) Long read (9 kb) and short read (150 bp) PCR products derived from genomic DNA extracted from HeLa cells expressing GFP or survivin–GFP (SVN–GFP) (A), or upon survivin knockdown with siRNA (SVN siRNA) (C), as well as in normal fibroblast MRC5 cells (E). Long read fragments were reduced in survivin–GFP-expressing HeLa cells, but increased after SVN siRNA. In comparison, in MRC5 cells no change was observed after survivin depletion. (B,D,F) Semi-quantitative analysis of the long read band intensity normalised to the short read 150 bp product. Results are mean±s.e.m.; n=3. ***P<0.001; ****P<0.0001 (two-way ANOVA).

Survivin expression increases glucose consumption and lactate production

As survivin overexpression was found to reduce OxPhos, our final question was whether cancer cells compensated for this reduction by increasing glycolytic respiration. To test this, we used luciferase-based assays to measure glucose consumption and lactate production. Survivin–GFP HeLa cells had a significantly lower glucose concentration (Fig. 8G) and higher rate of lactate production (Fig. 8H) compared to GFP-expressing cells 2 h post-seeding. Moreover, the rates at which glucose was consumed and lactate concentration rose was significantly higher than those observed in GFP cells. As both cell lines grew at the same rate (Fig. 8I), we conclude that the differences observed were due primarily to metabolic adjustments and not differences in proliferation.

DISCUSSION

Survivin is an essential protein that is deregulated in cancer, becoming present throughout the cell cycle, rather than being confined to G2 and M phases (Barrett et al., 2009). In transformed cells, in interphase it is predominantly cytoplasmic, shuttling between the cytoplasm and nucleus in a CRM1 (exportin)-dependent manner (Colnaghi et al., 2006; Engelsma et al., 2007; Stauber et al., 2007). Cytoplasmic survivin inhibits apoptosis, and it has been suggested that prior residence in the mitochondria can enhance this activity (Dohi et al., 2007). Consistent with previous studies (Dohi et al., 2004, 2007; Hagenbuchner et al., 2013, 2016; Rivadeneira et al., 2015), we found that survivin only accesses the mitochondria of transformed cells. Although survivin is essential, presumably its mitochondrial residence is not, and constitutes a gain of function over its normal roles.

In this study, we tested the hypothesis that survivin interferes with mitochondrial homeostasis and alters respiratory dependence in cancer cells. Mitochondria are dynamic organelles that regulate cellular metabolism and survival. The opposing pathways of mitochondrial biogenesis and autophagic degradation control their quantity and quality. Combined with fusion and fission, these mechanisms govern mitochondrial activity (Palikaras et al., 2015), and alterations to any one of these processes have been linked to ageing and disease (Redmann et al., 2014). In cancer cells, these processes are often deregulated, consequently mitochondrial health is compromised; mtDNA harbouring mutations accumulates, respiratory efficiency declines, and ultimately cells switch from OxPhos to glycolytic dependence (Merz and Westermann, 2009; Sumpter et al., 2016). OxPhos itself plays a major role in mtDNA damage as it produces ROS that continuously bombard the mtDNA, causing lesions (Ray et al., 2012; Sabharwal and Schumacker, 2014). Healthy cells respond to this damage by removing the affected sections of mitochondria using a selective form of autophagy called mitophagy (see Fig. S7).

Mitophagy commences with mitochondrial fission, which produces asymmetrical daughter mitochondria, one with an increased membrane potential that can fuse with healthy mitochondria (Twig et al., 2008a), and one with a depolarised membrane that is targeted for mitophagy (Elmore et al., 2001; Nicholls, 2004). Depolarisation of the OMM of defunct mitochondria stabilises the serine/threonine kinase PINK1, which

Journal of Cell Science (2020) 133, jcs247379. doi:10.1242/jcs.247379

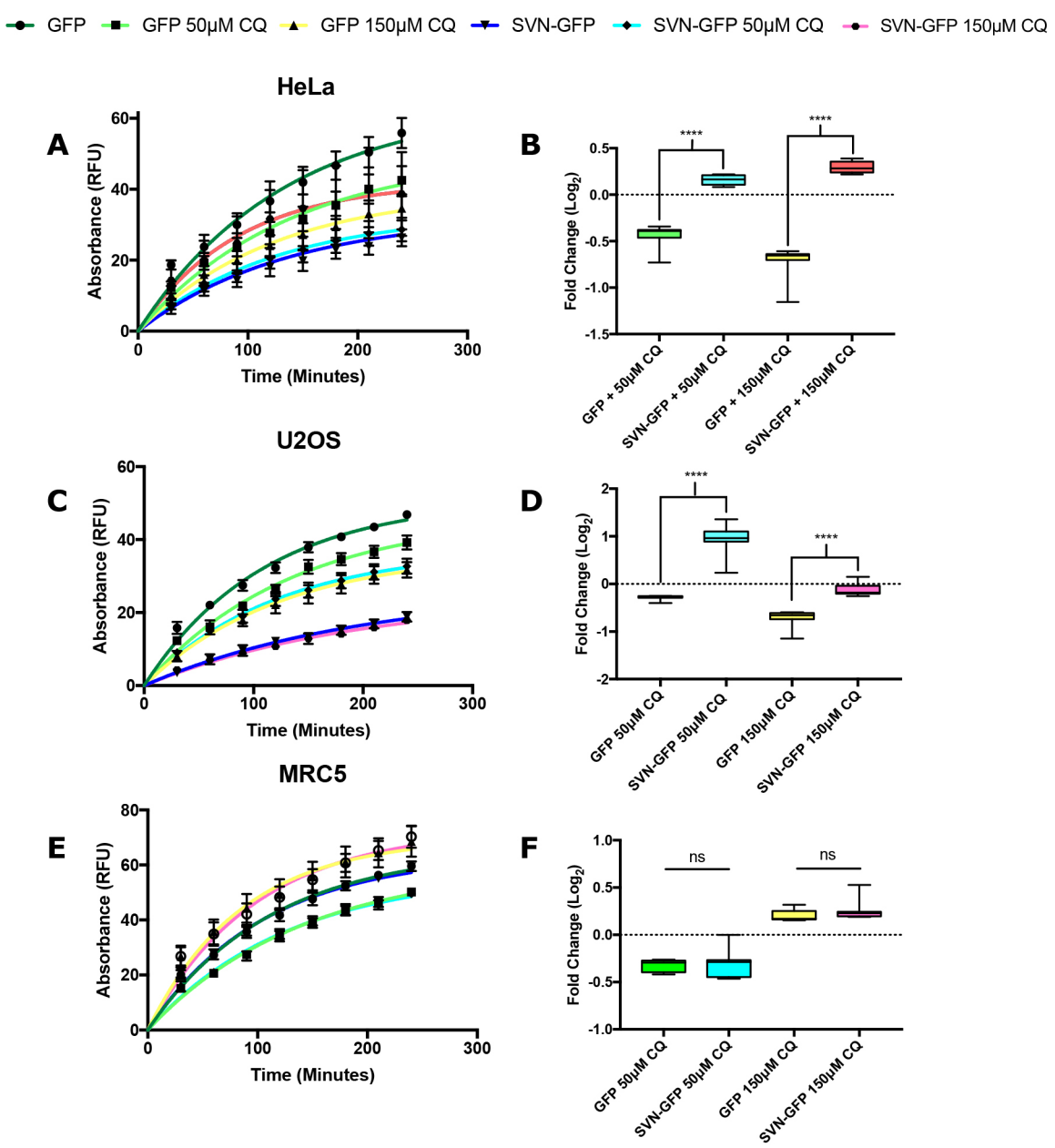

Fig. 7. Effect of CQ treatment on mitochondrial respiration. Mitochondria isolated from (A,B) HeLa, (C,D) U2OS or (E,F) MRC5 cells expressing GFP or survivin–GFP (SVN–GFP) were plated with the addition of resazurin medium with or without 50 µM or 150 µM CQ, and metabolism was assessed by determining the absorption of the produced resorufin, presented in relative fluorescence units (RFU) every 30 min for 4 h. Data was plotted as a graph (A,C,E), and analysed to calculate the fold change (log_2) in resorufin absorbance compared to GFP control (B,D,F). Non-linear regression shows no line fits between GFP curves in HeLa (A) or U2OS (C) mitochondria, whereas no change or a statistical increase is seen in SVN–GFP cells treated in response to CQ treatment (P<0.001, or P=0.1405 and 0.4825, respectively). (B,D) Mitochondria isolated from GFP-expressing HeLa and U2OS cells display a greater negative fold change in resorufin absorbance post-CQ treatment compared to SVN–GFP mitochondria. (E,F) Mitochondrial isolated from MRC5 expressing GFP or SVN–GFP display the same fold change in resorufin fluorescence post-CQ treatment (F). Non-linear regression analysis shows line fits for both MRC5 GFP and SVN–GFP with 50 µM or 150 µM CQ (E). Results in A, C and E are mean±s.e.m., n=3; results in B, D and F are shown as box-and-whisker plots (n=3), where the box represents the 25–75th percentiles, and the median is indicated. The whiskers show the range from minimum to maximum value. ****P<0.0001; ns, not significant (two-way ANOVA).

phosphorylates the E3-ligase Parkin at Ser65, and activates it. Parkin then accumulates at the OMM (Vives-Bauza et al., 2010; Youle and Narendra, 2011) where it mediates ubiquitylation of VDAC1 (Kazlauskaite et al., 2014). In turn VDAC1 ubiquitylation stimulates translocation of the autophagic adaptor protein, p62 (also known as SQSTM1) to the mitochondria, which signals their engulfment by pre-autophagosomes via interaction with LC3 family proteins (Lee et al., 2010; East and Campanella, 2016).

As indicated by increased expression of VDAC, mtDNA copy number and MitoTracker Green pixel area, ectopic expression of survivin caused an increase in total mitochondrial mass. We also noted that VDAC was being affected post-translation, while FIS1 levels, which decreased when survivin levels were elevated, were affected by transcriptional repression. We have also found that survivin does not increase mitochondrial biogenesis, nor does it alter mitochondrial dynamics, which contrasts with findings in

Journal of Cell Science (2020) 133, jcs247379. doi:10.1242/jcs.247379

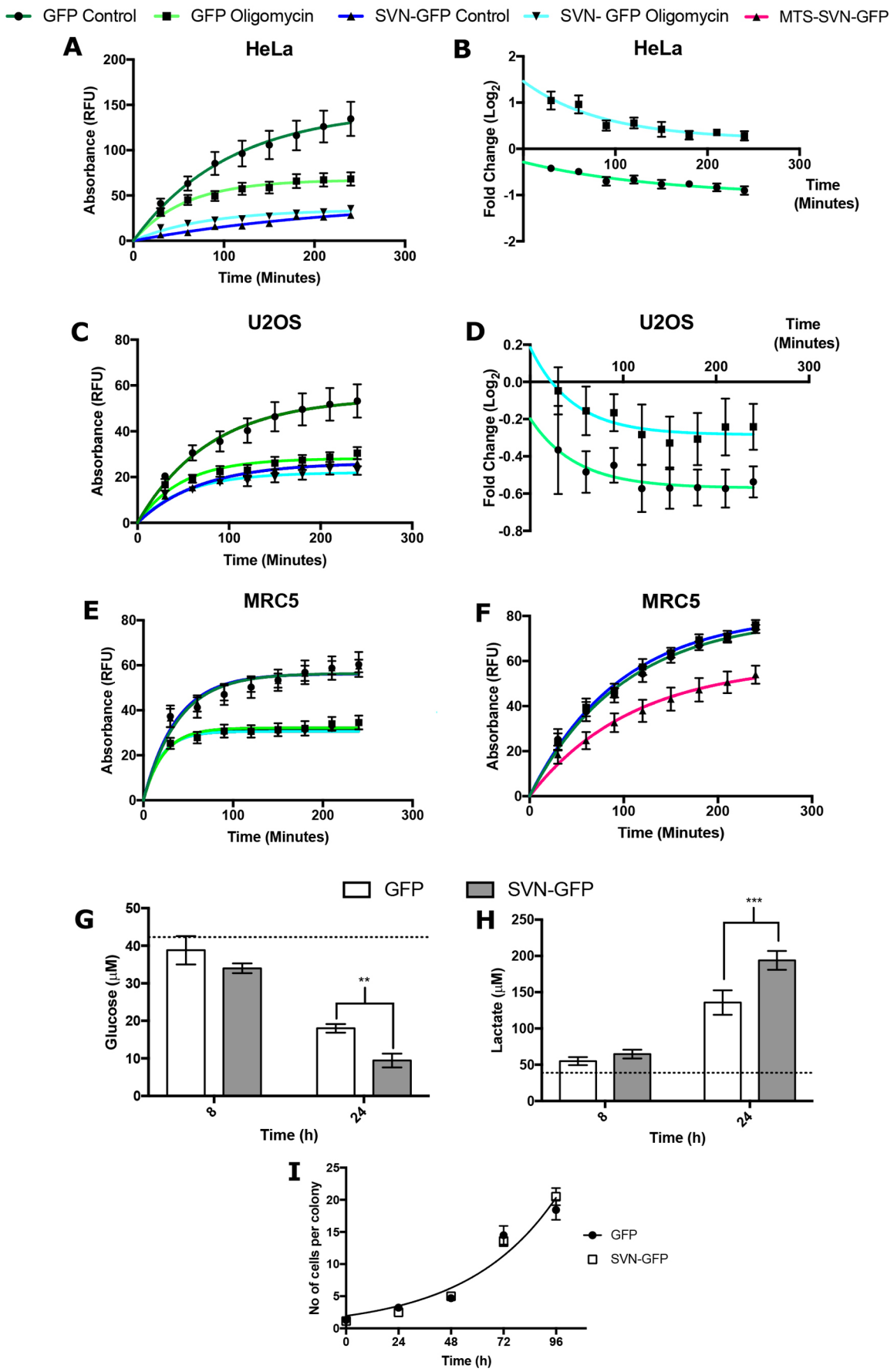

Fig. 8. See next page for legend.

Journal of Cell Science (2020) 133, jcs247379. doi:10.1242/jcs.247379

Fig. 8. Analysis of mitochondrial respiration, and response to oligomycin and lactate production. Mitochondria were isolated from (A,B) HeLa, (C,D) U2OS or (E) MRC5 cells expressing GFP or survivin–GFP (SVN–GFP) and plated in resazurin medium with or without oligomycin, and metabolism was assessed by determining the absorption of the produced resorufin, presented in relative fluorescence units (RFU) every 30 min for 4 h. Data was plotted as a graph (A,C,E), and analysed to calculate the fold change (log_2) in resorufin absorbance compared to GFP control (B,D). In A and C, non-linear regression analysis demonstrates that SVN–GFP mitochondria metabolise resazurin to a lesser degree than GFP mitochondria (P<0.0001). In addition, oligomycin treatment significantly reduces metabolism in the GFP control (P<0.001 and P<0.0001 for A and C, respectively), whereas SVN–GFP mitochondria are unaffected. In comparison, a single curve fitted to the untreated and treated datasets shown in E [GFP versus SVN–GFP, GFP+oligomycin versus SVN–GFP+oligomycin (P=0.9808 and 0.4123, respectively)]. (B,D) Non-linear regression analysis reveals mitochondria from HeLa and U2OS display a greater fold change in resorufin fluorescence with oligomycin treatment compared to SVN–GFP mitochondria in B and D (P<0.001 and P<0.0001, respectively). (F) Mitochondria isolated from MRC5 cells expressing GFP, SVN–GFP or MTS-SVN–GFP were metabolically analysed as above. Non-linear regression analysis demonstrates that MTS-SVN–GFP expression reduces resorufin fluorescence in comparison to GFP or SVN–GFP (P<0.0001). (G) Glucose consumption of 10,000 cells was measured over 72 h using a glucose-Glo assay. **P<0.01 (two-way ANOVA test at 24 h). Regression analysis to analyse difference in rate of change; the F test proves significant difference (P=0.0176). (H) Lactate production was measured as for G using a lactate-Glo assay. ***P<0.001 (two-way ANOVA test at 24 h). Regression analysis and F-test proves significant differences (P=0.0029). Dotted line shows glucose or lactate concentration at 0 h. n=2 (internally in triplicate). (I) HeLa cells expressing GFP and SVN–GFP grow at the same rate. 200 HeLa cells were seeded and the number of cells per colony counted over 72 h; n=3 (internally in triplicate). All quantitative results are mean±s.e.m.

neuroblastoma (Hagenbuchner et al., 2013). Subsequent data suggest that in the cancer cells observed here, survivin increases mitochondrial mass by preventing mitochondrial translocation of Parkin, which arrests the mitophagic process by preventing lysosomes from colocalising with, and degrading defective mitochondria (Fig. S7). Moreover, through the use of a bona fide mitochondrial-targeting signal from cytochrome *c* oxidase subunit VIIIA (MTS-SVN–GFP) we were able to force non-cancerous MRC5 cells to behave like the cancerous cells, and thus to demonstrate that the changes that we have reported can be attributed specifically to the presence of survivin in the mitochondria.

In addition to the increase in mitomass, we found that cancerous cells expressing survivin had poor quality mtDNA, and that survivin suppressed OxPhos and increased respiratory dependency on glycolysis in these cells. Additionally, through the use of MTS-SVN–GFP we were able to reduce mitochondrial metabolism in non-cancerous MRC5 cells, which is similar to the effect of wild-type survivin in HeLa cells. It is well documented that when mitophagy is inhibited, mitochondria with mtDNA lesions accumulate within the cell. This can directly impact the activity of mtDNA-encoded proteins, notably members of the electron transport chain (Sumpter et al., 2016), which directly impacts mitochondrial metabolism. Mitophagy can be artificially blocked using general autophagy inhibitors, such as CQ, which has been shown to reduce mitochondrial metabolism in the described manner (Redmann et al., 2017). Here, we saw no further reduction in the respiration of mitochondria isolated from survivin–GFP-expressing cancer cells after treatment with CQ, therefore allowing us to conclude that survivin modifies mitochondrial metabolism specifically due to alterations to mitophagy. Survivin inhibits mitophagy, causing an accumulation of respiratory defective organelles, which in turn reduces OxPhos (Redmann et al., 2017). Moreover, as OxPhos was altered to the same degree by CQ treatment in MRC5 cells irrespective of survivin expression, we conclude that this change is due to the mitochondrial pool of survivin.

When determining where survivin acts in the mitophagic pathway, we found that mitochondrial fragmentation, OMM depolarisation, PINK1 stabilisation and its interaction with the E3 ubiquitin ligase Parkin was not affected. Instead survivin prevents the recruitment of Parkin to the mitochondria. It has previously been reported that survivin inhibits the activities of PINK1 and Parkin, and that this response causes survivin degradation (Hagenbuchner et al., 2016). While our study also links survivin and Parkin, we offer a slightly alternative interpretation – that rather than causing its own demise, survivin inhibits mitophagy by preventing Parkin from translocating to the mitochondria, and the resulting accumulation of mitochondria with damaged mtDNA ultimately forces the cell to switch from oxidative phosphorylation to glycolysis. As we have previously shown that survivin can inhibit autophagic flux (Humphry and Wheatley, 2018), we suggest that survivin can interfere with mitophagy both by inhibiting Parkin recruitment to the OMM, and later, preventing flux (Fig. S7). Although a less efficient means of respiration, glycolysis produces less ROS, and thus, in addition to the initial survival response, this switch can provide cancer cells with a further survival advantage.

Our findings with survivin mirror these described by Hollville et al. (2014), in a series of experiments examining the role of the apoptosis inhibitor Bcl-2. Accordingly, treatment with the Bcl-2 inhibitor Navitoclax partially recovered the translocation of Parkin to the mitochondria, suggesting survivin acts in this process through a collaboration with Bcl-2.

Finally, as none of these changes occurred in normal fibroblasts in which survivin is not mitochondrial, and in fact forcing survivin into the mitochondria of these cells increases mitomass and decreases metabolism, we conclude that the effects are exclusive to cancer cells and can be attributed solely to the mitochondrial pool of survivin. The targeting of mitochondrial survivin and the metabolic alterations it provides cancerous cells, could therefore offer a distinct opportunity to develop novel therapeutic treatments with reduced off target effects in non-cancerous cell lines.

MATERIALS AND METHODS

All reagents were obtained from Sigma unless specified.

Human cell culture

Human epithelial carcinoma cells (HeLa, ATCC), osteosarcoma (U2OS) and normal lung fibroblasts (MRC5; Medical Research Council Strain 5, Genome and Stability Centre, Sussex), were cultured in 5% CO_2 at 37°C with humidity in Dulbecco's modified Eagle's medium (DMEM, Gibco, Invitrogen) supplemented with 4 mM L-glutamine, 10% fetal calf serum (FCS, ThermoScientific), 244 µM penicillin and 172 µM streptomycin. Derivative lines expressing GFP or survivin–GFP were maintained under the selection pressure of 1 mM G418 (Fisher). Experiments were carried out on cells within 30 passages. Treatments: 10 µM FCCP for 3 h or 50, 100 or 150 µM CQ for the times indicated.

DNA and siRNA transfections

Cells were seeded into a relevant dish or imaging chamber in antibiotic free medium, incubated for 12 h before transfection and left for ∼48 h before use. DNA transfections were performed using Torpedo Transfection reagent (Ibidi) and 0.3 µg of relevant DNA construct (see Table S1), as per the manufacturer's guidelines. siRNA transfections were performed using HiPerfect transfection reagent (Qiagen) and 75 ng of relevant siRNA, as per the manufacturer's instruction. The mCherry–Parkin construct was a gift from Professor Seamus Martin, Smurfit Institute, Trinity College Dublin, Ireland. The GST–Parkin-WT construct was from Addgene (#45969, deposited by Kalle Gehring; Trempe et al., 2013).

Journal of Cell Science (2020) 133, jcs247379. doi:10.1242/jcs.247379

Cell counting assay

Cells were seeded at a density of 200 cells per 10 cm Petri dish, and the number of cells in individual colonies after 8, 24, 48 and 72 h.

Immunoblotting

Protein samples were separated according to standard procedures using 12% acrylamide SDS-PAGE gels, in running buffer [25 mM Tris, 192 mM glycine, 0.1% (w/v) SDS] and transferred onto a 0.22 µM nitrocellulose membrane (BIOTRACE, PALL life sciences) using transfer buffer (24 mM Tris, 195 mM glycine, 0.1% SDS, 10% methanol). Post-transfer membranes were blocked with 5% non-fat milk [Marvel, in PBS +0.1% Tween 20 (PBST)] then incubated with appropriate primary antibody overnight at 4°C, washed three times with PBST, then incubated in the appropriate horseradish-peroxidase conjugated secondary antibody in 5% non-fat milk. EZ-ECL chemilluminescence detection reagent was then added (Geneflow) and membrane exposed to detection film (Roche). Details of primary antibodies are shown in Table S3.

Immunoblots were quantified using Fiji software. Band intensity peaks were measured and combined into sample groups for each condition. Within each pool, intensity values for each protein were expressed as a percentage of the loading control average and then as a percentage of the control protein average. The final expression value was presented as a decimal and transformed as a function of a base 2 logarithm ($\log_2$).

Mitochondrial DNA lesion assay

2×10^6 cells were washed with PBS and harvested by scraping. Genomic DNA was extracted using the GeneJET genomic DNA purification kit (Thermo Scientific #K0721) according to the manufacturer's instructions.

To determine mitochondrial DNA integrity, a PCR was performed on gDNA samples using 6 ng of template gDNA, 250 µM dNTPs, 500 nM of either a short read [tRNA(LEU)] or a long read (LR-mtDNA) primer mix, 0.02 U/µl Q5 DNA polymerase and 1X Q5 reaction buffer. Long read PCR was aided by the addition of 10 ng/µl BSA. PCR products were then run on a 0.8% agarose gel, and quantified using Fiji software as described for immunoblots. See Table S2 for details of primers.

RNA extraction

7×10^6 cells were harvested by scraping into 0.2 ml of medium, 1 ml TRI-reagent was added and the samples incubated (5 min at room temperature). 200 µl 1-bromo-3-chloropropane [BCP; 11.76% (v/v) in TRI reagent and residual DMEM] was then added and the sample incubated for a further 3 min at room temperature before centrifugation (10,000 ***g***, Labnet, Prism R). The upper (colourless) layer was removed and incubated overnight at −20°C in acidifed isopropanol solution [256 mM sodium acetate pH 4 and 36% isopropanol (v/v)]. Samples were centrifuged at 17,000 ***g*** for 15 min at 4°C and pellets washed in 70% ethanol. Samples were treated with RNase-free DNase-I (Qiagen) according to the manufacturer's instructions. RNA was isolated by phenol-chloroform-isoamyl-alchohol [50% phenol-chloroform-isoamy-alchohol (v/v) 125:24:1] in dH_2O. Samples were vigorously shaken and incubated for 3 min at room temperature before centrifugation (11,000 ***g*** for 9 min at 12°C). The upper aqueous phase was transferred to a fresh tube and incubated overnight at −20°C in acidified ethanol solution [323 mM sodium acetate pH 5.2 and 65% ethanol (v/v)]. Precipitated samples were washed in 70% ethanol, pellets dried, dissolved in dH_2O and RNA concentration determined by spectrophotometry (Nanodrop 2000, Thermo Scientific).

Comparative qPCR

qPCR was performed using iTaq™ Universal SYBR® Green Supermix (BIORAD) as per the manufacturer's instructions on a qPCR thermocycler (7500 fast real-time qPCR, Applied Biosciences). gDNA samples were analysed at a final concentration of 200 pg/µl with 500 nM primers (see Table S2). Data sets were analysed, and reference genes verified using the Pfaffl method (see https://gene-quantification.de/pfaffl-rel-quan-book-ch3.pdf) and REST software (QIAGEN).

Subcellular fractionation

Cells grown to 80–90% confluence in 15 cm^2 Petri dishes were washed and scraped into PBS and pelleted at 300 ***g*** for 3 min, before re-suspension in 2 ml homogenisation buffer (200 mM mannitol, 70 mM sucrose, 1 mM EGTA and 10 mM HEPES, pH 7.5) supplemented with protease and kinase inhibitors. Lysates were prepared in a glass homogeniser (Teflon), a sample taken as WCE, before spinning at 1000 ***g***, 4°C for 5 min. Supernatants were transferred to a fresh tube (mitochondrial/cytoplasmic fraction) and centrifuged at 10,000 ***g***, 4°C for 15 min to pellet mitochondria before re-suspension in homogenisation buffer. Protein concentration was then measured by means of a Bradford assay and samples were boiled in SDS sample buffer, and 20 µg protein loaded onto an SDS-PAGE gel for analysis.

Resazurin assays

Mitochondrial metabolism assays were performed using 20 µg of isolated mitochondria resuspended in Locke's buffer [154 mM NaCl, 5.6 mM KCl (BDH), 2.3 mM $CaCl_2$ (Fisher), 1 mM $MgCl_2$, 3.6 mM $NaHCO_3$, 5 mM glucose and 5 mM HEPES pH 7.5 (BDH)] and plated into one well of a black 96-well plate (CLS3904). 40 µM resazurin was then added to each sample to make a final concentration of 20 µM and plates were then incubated at 37°C with 5% CO_2. Absorbance was then read at 595 nm every 30 min for 4 h and compared to that of 20 µM resazurin blank controls (FluoStar Galaxy).

Cell death curves were performed on 50,000 HeLa cells expressing GFP, pre-treated with and without 1 µM of the BCL-2 inhibitor Navitoclax for 16 h. Cells were treated with 0, 0.02, 0.08, 0.32, 1.28 or 2.56 J of UV, left for 24 h, 20 µM of resazurin added and plates incubated at 37°C with 5% CO_2 for 1 h. Absorbance was read at 595 nm and compared to 20 µM resazurin control.

Glucose-Glo and Lactate-Glo assay

10,000 HeLa cells were plated per well of a 96 well plate in 100 µl DMEM (Gibco 11054001) containing 5.6 mM glucose, 2 mM glutamine and supplemented with 10% FCS. Medium-only wells acted as controls. At 8, 24, 48 and 72 h post-plating, 2.5 µl of medium was removed from each sample, diluted in 97.5 µl of PBS and frozen until needed. On the day of assay, samples were thawed and diluted a further 2.5×, and 50 µl of diluted medium added to a white 96-well plate (CLS3610) before the addition of 50 µl of lactate/glucose detection reagent (Promega). Plates were incubated for 1 h at room temperature and luminescence recorded (Glowmax Luminometer, Promega) and then compared to glucose/lactate standards to determine relevant concentrations.

Live-cell fluorescence imaging

To visualise active mitochondria, cells were grown overnight in 8-chambered micro-slides (Ibidi). Cells were stained to visualise mitochondria using either 500 nM MitoTracker Red CMXRos, MitoTracker Deep Red FM or 200 nM MitoTracker Green FM (Invitrogen), and Nucblue to visualise DNA (Thermo Fischer Scientific) in Phenol Red-free CO_2-independent medium (DMEM, Invitrogen) supplemented with 2 mM L-glutamine and 10% FCS, for 15 min at 37°C.

Mitochondrial membrane potential assay

HeLa or MRC5 cells were seeded into Ibidi 8-chambered chambers at ∼24 h before imaging and, once adherent, were incubated in DMEM without Phenol Red (D1145) supplemented with 4 mM L-glutamine and 25 mM HEPES. At 15 min before imaging, cells were stained with 1 drop of Nucblue (Life Technologies), 100 nM MitoTracker Green FM and 100 nM MitoTracker Deep Red FM or 200 µM tetramethylrhodamine ethyl ester perchlorate (TMRE, AAT Bioquest). Immediately before imaging, stains were washed off by replacing medium with Phenol Red-free CO_2-independent complete DMEM.

Image acquisition and processing

Imaging was performed using an inverted (DMRIB Olympus, Delta Vision Elite) microscope with a 60× (NA1.4, oil) objective. Single-plane images were acquired, de-convolved using inbuilt software on the Delta-vision, and saved as TIFF files. Image pixel intensity was quantified in Fiji using a fully automated macro, which was programmed first to threshold each channel to a set scale defined by the user, and then measure the average signal intensity of each channel. Colocalisation analysis was performed using a similar macro that after thresholding images, was then programmed to analyse the percentages of pixels that spatially colocalised with similar intensity

between the two channels. Datasets were then analysed in the GraphPad Prism software.

Protein purification

The relevant pGEX construct was transformed into BL21 (DE3) pLysS cells using a standard heat-shock technique and plated onto ampicillin (100 mg/ml) LB agar. Starter colonies were grown from picked single colonies and used to inoculate larger cultures at 37°C until OD_{600}=0.6. Protein expression was induced through the addition of 0.5 mM isopropyl β-d-1-thiogalactopyranoside (IPTG) (25 µM for GST–Parkin) and 500 µM $ZnCl_2$, and cultures left overnight at 20°C (16°C for GST–Parkin), rocking (220 rpm). Cells were harvested by centrifugation at 3200 ***g*** and washed with TBS before resuspension in 5 ml TBS supplemented with 2 mM β-mercaptoethanol, 1 µg/ml CLAP, DNase and 10 mM $MgCl_2$. Samples were lysed by sonication and spun at 48,000 ***g*** for 30 min. Supernatant was added to washed Glutathione Sepharose 4B beads (GE Life Sciences, 17075604) for 1 h at 4°C, and then collected by centrifugation at 300 ***g*** for 5 min. Samples were eluted using elution buffer (10 mM reduced glutathione and 50 mM Tris-HCl pH 8.0), and glutathione removed using wash buffer (50 mM Tris-HCl and 150 mM NaCl) overnight in dialysis tubing.

GST pulldown assay

200 µl washed Glutathione Sepharose beads were bound to 1 mg purified GST-tagged protein, incubated rotating for 1 h at 4°C and then pelleted by centrifugation at 500 ***g*** for 15 minutes. Whole-cell extracts of interest were prepared in RIPA buffer (20 mM Tris-HCl pH 8.0, 137 mM NaCl, 1% NP-40 and 0.1% Tween) and incubated with beads for 2 h at 4°C. Beads were then washed in RIPA wash buffers 1 (50 mM Tris-HCl pH 8.0, 150 mM NaCl, 1% NP-40 and 0.5 mM EDTA), 2 (50 mM Tris-HCl pH 8.0, 150 mM NaCl and 1% NP-40) and 3 (50 mM Tris-HCl pH 8.0 and 1% NP-40) for 15 min, then boiled in 2× SDS loading dye.

Acknowledgements

We thank Dr Sophie Rochette for technical support, Alex Fezovich for generating the MTS-survivin cell lines and his assistance with Fiji, James Grey for his expertise in qPCR data acquisition and analysis and Prof. Seamus Martin for mCherry–PARKIN.

Competing interests

The authors declare no competing or financial interests.

Author contributions

Conceptualization: A.R.T., S.P.W.; Methodology: A.R.T., S.P.W.; Validation: A.R.T., S.P.W.; Investigation: S.P.W.; Data curation: A.R.T.; Writing - original draft: A.R.T.; Writing - review & editing: S.P.W.; Visualization: A.R.T., S.P.W.; Supervision: S.P.W.; Project administration: S.P.W.; Funding acquisition: S.P.W.

Funding

A.R.T. was supported by a Biotechnology and Biological Sciences Research Council studentship.

Supplementary information

Supplementary information available online at
https://jcs.biologists.org/lookup/doi/10.1242/jcs.247379.supplemental

Peer review history

The peer review history is available online at
https://jcs.biologists.org/lookup/doi/10.1242/jcs.247379.reviewer-comments.pdf

References

Balaban, R. S., Nemoto, S. and Finkel, T. (2005). Mitochondria, oxidants, and aging. *Cell* **120**, 483-495. doi:10.1016/j.cell.2005.02.001

Barrett, R. M. A., Osborne, T. P. and Wheatley, S. P. (2009). Phosphorylation of survivin at threonine 34 inhibits its mitotic function and enhances its cytoprotective activity. *Cell Cycle* **8**, 278-283. doi:10.4161/cc.8.2.7587

Carvalho, A., Carmena, M., Sambade, C., Earnshaw, W. C. and Wheatley, S. P. (2003). Survivin is required for stable checkpoint activation in taxol-treated HeLa cells. *J. Cell Sci.* **116**, 2987-2998. doi:10.1242/jcs.00612

Chatterjee, A., Dasgupta, S. and Sidransky, D. (2011). Mitochondrial subversion in cancer. *Cancer Prevent. Res.* **4**, 638-654. doi:10.1158/1940-6207.CAPR-10-0326

Chourasia, A. H., Boland, M. L. and Macleod, K. F. (2015). Mitophagy and cancer. *Cancer Metab.* **3**, 4. doi:10.1186/s40170-015-0130-8

Colnaghi, R., Connell, C. M., Barrett, R. M. A. and Wheatley, S. P. (2006). Separating the anti-apoptotic and mitotic roles of survivin. *J. Biol. Chem.* **281**, 33450-33456. doi:10.1074/jbc.C600164200

Dispersyn, G., Nuydens, R., Connors, R., Borgers, M. and Geerts, H. (1999). Bcl-2 protects against FCCP-induced apoptosis and mitochondrial membrane potential depolarization in PC12 cells. *Biochim. Biophys. Acta General Subjects* **1428**, 357-371. doi:10.1016/S0304-4165(99)00073-2

Dohi, T., Beltrami, E., Wall, N. R., Plescia, J. and Altieri, D. C. (2004). Mitochondrial survivin inhibits apoptosis and promotes tumorigenesis. *J. Clin. Investig.* **114**, 1117-1127. doi:10.1172/JCI200422222

Dohi, T., Xia, F. and Altieri, D. C. (2007). Compartmentalized phosphorylation of IAP by protein kinase A regulates cytoprotection. *Mol. Cell* **27**, 17-28. doi:10.1016/j.molcel.2007.06.004

East, D. A. and Campanella, M. (2016). Mitophagy and the therapeutic clearance of damaged mitochondria for neuroprotection. *Int. J. Biochem. Cell Biol.* **79**, 382-387. doi:10.1016/j.biocel.2016.08.019

Elmore, S. P., Qian, T., Grissom, S. F. and Lemasters, J. J. (2001). The mitochondrial permeability transition initiates autophagy in rat hepatocytes. *FASEB J.* **15**, 2286-2287. doi:10.1096/fj.01-0206fje

Engelsma, D., Rodriguez, J. A., Fish, A., Giaccone, G. and Fornerod, M. (2007). Homodimerization antagonizes nuclear export of survivin. *Traffic* **8**, 1495-1502. doi:10.1111/j.1600-0854.2007.00629.x

Escuín, D. and Rosell, R. (1999). The anti-apoptosis survivin gene and its role in human cancer: an overview. *Clin. Lung Cancer* **1**, 138-143. doi:10.3816/CLC.1999.n.011

Fortugno, P., Wall, N. R., Giodini, A., O'Connor, D. S., Plescia, J., Padgett, K. M., Tognin, S., Marchisio, P. C. and Altieri, D. C. (2002). Survivin exists in immunochemically distinct subcellular pools and is involved in spindle microtubule function. *J. Cell Sci.* **115**, 575-585. Available at: http://www.ncbi.nlm.nih.gov/pubmed/11861764 (Accessed: 23 April 2019).

Hagenbuchner, J., Kuznetsov, A. V., Obexer, P. and Ausserlechner, M. J. (2013). BIRC5/Survivin enhances aerobic glycolysis and drug resistance by altered regulation of the mitochondrial fusion/fission machinery. *Oncogene* **32**, 4748-4757. doi:10.1038/onc.2012.500

Hagenbuchner, J., Kiechl-Kohlendorfer, U., Obexer, P. and Ausserlechner, M. (2016). BIRC5/Survivin as a target for glycolysis inhibition in high-stage neuroblastoma. *Oncogene* **35**, 2052-2061. doi:10.1038/onc.2015.264

Hollville, E., Carroll, R. G., Cullen, S. P. and Martin, S. J. (2014). Bcl-2 family proteins participate in mitochondrial quality control by regulating Parkin/PINK1-dependent mitophagy. *Mol. Cell* **55**, 451-466. doi:10.1016/j.molcel.2014.06.001

Humphry, N. J. and Wheatley, S. P. (2018). Survivin inhibits excessive autophagy in cancer cells but does so independently of its interaction with LC3. *Biol. Open* **7**, bio037374. doi:10.1242/bio.037374

Jaiswal, P. K., Goel, A. and Mittal, R. D. (2015). Survivin: a molecular biomarker in cancer. *Indian J. Med. Res.* **141**, 389-397. doi:10.4103/0971-5916.159250

Jornayvaz, F. R. and Shulman, G. I. (2010). Regulation of mitochondrial biogenesis. *Essays Biochem.* **47**, 69-84. doi:10.1042/bse0470069

Kazlauskaite, A., Kondapalli, C., Gourlay, R., Campbell, D. G., Ritorto, M. S., Hofmann, K., Alessi, D. R., Knebel, A., Trost, M. and Muqit, M. M. K. (2014). Parkin is activated by PINK1-dependent phosphorylation of ubiquitin at Ser^{65}. *Biochem. J.* **460**, 127-141. doi:10.1042/BJ20140334

Lee, J.-Y., Nagano, Y., Taylor, J. P., Lim, K. L. and Yao, T.-P. (2010). Disease-causing mutations in parkin impair mitochondrial ubiquitination, aggregation, and HDAC6-dependent mitophagy. *J. Cell Biol.* **189**, 671-679. doi:10.1083/jcb.201001039

Merz, S. and Westermann, B. (2009). Genome-wide deletion mutant analysis reveals genes required for respiratory growth, mitochondrial genome maintenance and mitochondrial protein synthesis in Saccharomyces cerevisiae. *Genome Biol.* **10**, R95. doi:10.1186/gb-2009-10-9-r95

Morrison, D. J., Hogan, L. E., Condos, G., Bhatla, T., Germino, N., Moskowitz, N. P., Lee, L., Bhojwani, D., Horton, T. M., Belitskaya-Levy, I. et al. (2012). Endogenous knockdown of survivin improves chemotherapeutic response in ALL models. *Leukemia* **26**, 271-279. doi:10.1038/leu.2011.199

Nicholls, D. G. (2004). Mitochondrial membrane potential and aging. *Aging Cell* **3**, 35-40. doi:10.1111/j.1474-9728.2003.00079.x

Nunnari, J., Marshall, W. F., Straight, A., Murray, A., Sedat, J. W. and Walter, P. (1997). Mitochondrial transmission during mating in Saccharomyces cerevisiae is determined by mitochondrial fusion and fission and the intramitochondrial segregation of mitochondrial DNA. *Mol. Biol. Cell* **8**, 1233-1242. doi:10.1091/mbc.8.7.1233

Ott, M., Gogvadze, V., Orrenius, S. and Zhivotovsky, B. (2007). Mitochondria, oxidative stress and cell death. *Apoptosis* **12**, 913-922. doi:10.1007/s10495-007-0756-2

Palikaras, K., Lionaki, E. and Tavernarakis, N. (2015). Balancing mitochondrial biogenesis and mitophagy to maintain energy metabolism homeostasis. *Cell Death Differ.* **22**, 1399-1401. doi:10.1038/cdd.2015.86

Porporato, P. E., Filigheddu, N., Pedro, J. M. B.-S., Kroemer, G. and Galluzzi, L. (2017). Mitochondrial metabolism and cancer. *Cell Res.* **28**, 265-280. doi: 10.1038/cr.2017.155

Ray, P. D., Huang, B.-W. and Tsuji, Y. (2012). Reactive oxygen species (ROS) homeostasis and redox regulation in cellular signaling. *Cell. Signal.* **24**, 981-990. doi:10.1016/j.cellsig.2012.01.008

Redmann, M., Dodson, M., Boyer-Guittaut, M., Darley-Usmar, V. and Zhang, J. (2014). Mitophagy mechanisms and role in human diseases. *Int. J. Biochem. Cell Biol.* **53**, 127-133. doi:10.1016/j.biocel.2014.05.010

Redmann, M., Benavides, G. A., Berryhill, T. F., Wani, W. Y., Ouyang, X., Johnson, M. S., Ravi, S., Barnes, S., Darley-Usmar, V. M. and Zhang, J. (2017). Inhibition of autophagy with bafilomycin and chloroquine decreases mitochondrial quality and bioenergetic function in primary neurons. *Redox Biol.* **11**, 73-81. doi:10.1016/j.redox.2016.11.004

Rivadeneira, D. B., Caino, M. C., Seo, J. H., Angelin, A., Wallace, D. C., Languino, L. R. and Altieri, D. C. (2015). Survivin promotes oxidative phosphorylation, subcellular mitochondrial repositioning, and tumor cell invasion. *Sci. Signal.* **8**, ra80. doi:10.1126/scisignal.aab1624

Sabharwal, S. S. and Schumacker, P. T. (2014). Mitochondrial ROS in cancer: initiators, amplifiers or an Achilles' heel? *Nat. Rev. Cancer* **14**, 709-721. doi:10.1038/nrc3803

Shaid, S., Brandts, C. H., Serve, H. and Dikic, I. (2013). Ubiquitination and selective autophagy. *Cell Death Differ.* **20**, 21-30. doi:10.1038/cdd.2012.72

Stauber, R. H., Mann, W. and Knauer, S. K. (2007). Nuclear and cytoplasmic survivin: molecular mechanism, prognostic, and therapeutic potential. *Cancer Res.* **67**, 5999-6002. doi:10.1158/0008-5472.CAN-07-0494

Sumpter, R., Sirasanagandla, S., Fernández, Á. F., Wei, Y., Dong, X., Franco, L., Zou, Z., Marchal, C., Lee, M. Y., Clapp, D. W. et al. (2016). Fanconi anemia proteins function in mitophagy and immunity. *Cell* **165**, 867-881. doi:10.1016/j.cell.2016.04.006

Trempe, J.-F., Sauvé, V., Grenier, K., Seirafi, M., Tang, M. Y., Ménade, M., Al-Abdul-Wahid, S., Krett, J., Wong, K., Kozlov, G. et al. (2013). Structure of parkin reveals mechanisms for ubiquitin ligase activation. *Science* **340**, 1451-1455. doi:10.1126/science.1237908

Twig, G. and Shirihai, O. S. (2011). The interplay between mitochondrial dynamics and mitophagy. *Antioxid Redox Signal.* **14**, 1939-1951. doi:10.1089/ars.2010.3779

Twig, G., Elorza, A., Molina, A. J. A., Mohamed, H., Wikstrom, J. D., Walzer, G., Stiles, L., Haigh, S. E., Katz, S., Las, G. et al. (2008a). Fission and selective fusion govern mitochondrial segregation and elimination by autophagy. *EMBO J.* **27**, 433-446. doi:10.1038/sj.emboj.7601963

Twig, G., Hyde, B. and Shirihai, O. S. (2008b). Mitochondrial fusion, fission and autophagy as a quality control axis: the bioenergetic view. *Biochim. Biophys. Acta* **1777**, 1092-1097. doi:10.1016/j.bbabio.2008.05.001

van Gisbergen, M. W., Voets, A. M., Starmans, M. H. W., de Coo, I. F. M., Yadak, R., Hoffmann, R. F., Boutros, P. C., Smeets, H. J. M., Dubois, L. and Lambin, P. (2015). How do changes in the mtDNA and mitochondrial dysfunction influence cancer and cancer therapy? Challenges, opportunities and models. *Mutat. Res.* **764**, 16-30. doi:10.1016/j.mrrev.2015.01.001

Vander Heiden, M. G., Cantley, L. C. and Thompson, C. B. (2009). Understanding the Warburg effect: the metabolic requirements of cell proliferation. *Science* **324**, 1029-1033. doi:10.1126/science.1160809

Vara-Perez, M., Felipe-Abrio, B. and Agostinis, P. (2019). Mitophagy in cancer: a tale of adaptation. *Cells* **8**, 493. doi:10.3390/cells8050493

Vives-Bauza, C., Zhou, C., Huang, Y., Cui, M., de Vries, R. L. A., Kim, J., May, J., Tocilescu, M. A., Liu, W., Ko, H. S. et al. (2010). PINK1-dependent recruitment of Parkin to mitochondria in mitophagy. *Proc. Natl. Acad. Sci. USA* **107**, 378-383. doi:10.1073/pnas.0911187107

Warburg, O. (1956). On the origin of cancer cells. *Science* **123**, 309-314. doi:10.1126/science.123.3191.309

Westermann, B. (2010). Mitochondrial fusion and fission in cell life and death. *Nat. Rev. Mol. Cell Biol.* **11**, 872-884. doi:10.1038/nrm3013

Wheatley, S. P. and Altieri, D. C. (2019). Survivin at a glance. *J. Cell Sci.* **132**, jcs223826. doi:10.1242/jcs.223826

Yadav, N. and Chandra, D. (2013). Mitochondrial DNA mutations and breast tumorigenesis. *Biochim. Biophys. Acta* **1836**, 336-344. doi:10.1016/j.bbcan.2013.10.002

Youle, R. J. and Narendra, D. P. (2011). Mechanisms of mitophagy. *Nat. Rev. Mol. Cell Biol.* **12**, 9-14. doi:10.1038/nrm3028

Zaffagnini, G. and Martens, S. (2016). Mechanisms of selective autophagy. *J. Mol. Biol.* **428**, 1714-1724. doi:10.1016/j.jmb.2016.02.004